Pharm Res (2010) 27:1869–1883
DOI 10.1007/s11095-010-0185-8

RESEARCH PAPER

Characterisation and Prediction of Phase Separation in Hot-Melt Extruded Solid Dispersions: A Thermal, Microscopic and NMR Relaxometry Study

Sheng Qi • Peter Belton • Kathrin Nollenberger • Nigel Clayden • Mike Reading • Duncan Q. M. Craig

Received: 10 February 2010 / Accepted: 1 June 2010 / Published online: 29 June 2010

ABSTRACT

Purpose To develop novel analytical approaches for identifying both miscibility and phase separation in hot-melt extruded formulations.

Methods Felodipine-Eudragit® E PO solid dispersions were prepared using hot-melt extrusion. The fresh and aged formulations were characterised using scanning electron microscopy, differential scanning calorimetry, heat capacity (C_p) measurements using modulated temperature DSC and nuclear magnetic resonance relaxometry.

Results The solubility of the drug in polymer was predicted as being ≤10% w/w using a novel model proposed in this study. Freshly prepared HME formulations were found to show no evidence for phase separation despite drug loadings greatly in excess of this figure. Conventional DSC showed limitations in directly detecting phase separation. However, a novel use of C_p measurements indicated that extensive phase separation into crystalline domains was present in all aged samples, a conclusion supported by SEM studies. The NMR relaxometry study confirmed the existence of phase separation in all aged formulations and also allowed the estimation of separated domains sizes in different formulations.

Conclusions This study has presented a series of novel approaches for the identification, quantification and prediction of phase separation in HME formulations. Supersaturation of drug in the polymer caused the phase separation of the aged felodipine-Eudragit® E PO formulations.

KEY WORDS heat capacity · hot melt extrusion · miscibility · phase separation · supersaturation

S. Qi (✉) · M. Reading · D. Q. M. Craig
School of Pharmacy, University of East Anglia
Norwich, Norfolk NR4 7TJ, UK
e-mail: sheng.qi@uea.ac.uk

P. Belton · N. Clayden
School of Chemistry, University of East Anglia
Norwich, Norfolk NR4 7TJ, UK

K. Nollenberger
Evonik Röhm GmbH
Kirschenallee, 64293 Darmstadt, Germany

INTRODUCTION

Hot-melt extrusion (HME) has attracted increasing attention as a novel method for preparing solid dispersion formulations for poorly water-soluble drugs (1–6). More specifically, a significant improvement in the dissolution rate of drugs may be elicited by the formation of a solid dispersion via the hot-melt extrusion process, thereby potentially eliciting an improvement in bioavailability for BCS class II and IV drugs (2,7,8). While the solid dispersions may manifest as a range of binary systems, the formation of a solid solution of the drug within the polymer is generally regarded as being desirable mainly for reason of *in vitro* drug release performance (6,9–13). In the case of HME, the processing involves dispersion and fusion under mechanical stress. As it is well recognized that for many materials the solubility of a solute increases with temperature, it follows that for systems in which drug and the matrix material have a certain degree of miscibility, the melt extrusion process may promote the formation of supersaturated solid solution of the API. This could potentially lead to drug recrystallisation or separation from the HME formulation during storage. In the case of an immiscible drug and matrix polymer, if the processing temperature is above the melting temperature of the active ingredient, then solid dispersions of amorphous drug domains embedded in the polymer may be formed after

extrusion. Additionally, HME is a high stress process for the carrier material and the drug; as most of the matrix materials used are polymers and lipids, degradation of the polymer/lipid during the hot-melt extrusion process may occur (14,15). Therefore, accurate assessment of the physical and chemical stability of the hot-melt extruded formulations is essential.

As a consequence of the above, the development of reliable characterisation methods to provide accurate understanding of the physical state of the drug within the polymer is now a universally accepted need, particularly as this information can potentially be used to predict the physical stability of the HME formulations. The current routine solid-state characterisation methods of HME formulations include powder X-ray diffraction (PXRD), differential scanning calorimetry (DSC), and IR spectroscopy (1,3–5,16). These conventional analytical techniques can provide information on the overall average characteristics of the formulation but provide little or no spatially resolved information. A further disadvantage of some conventional methods, such as PXRD, is that the technique requires the original physical form of the hot-melt extruded product to be altered from, typically, cylinder-shaped extrudates to powders; the additional pulverisation process may alter the physical form of the drug or polymer. Conventional DSC also exhibits limitations in the characterisation of solid dispersion systems due to the dissolution of the drug in the molten matrix material below its melting point, causing diminution or disappearance of the melting peak which may be mistakenly considered to indicate solid solubility (17).

Typically, phase separation can manifest as the drug existing as crystalline or amorphous domains within the polymer. On a macroscopic scale, the distribution of the drug in the solid dispersion may be uniform but may also be uneven. For example, in systems containing amorphous drugs, the dispersions could contain spatially separated drug-rich and polymer-rich domains, indicating the presence of gradient of drug concentration in different regions of the dispersion (18). If the matrix material and the model drug have different melting points and are essentially immiscible, then solid dispersions containing crystalline drug domains are relatively easy to identify using standard DSC analysis, as the dissolution effect mentioned above will not be apparent. In cases where the crystalline drug dissolves in the molten matrix material during heating, we suggest that fast DSC (referring to systems whereby a rapid heating rate is used) may be more beneficial, since the high heating rate can reduce the time available for the kinetically hindered dissolution process.

Solid dispersions containing separated amorphous drug domains can potentially be characterised using DSC or, perhaps more usefully, MTDSC measurements if the polymer and the amorphous drug have different T_g values. However, if the T_g of the polymer and the amorphous drug are relatively similar, as may well be the case in practice, it is challenging to identify the two transitions belonging to the different components in the formulations. It may therefore be reasonably argued that the most problematic solid dispersions to characterise are those with similar T_g values and/or a significant degree of miscibility between the drug and matrix material. Unfortunately, our experience thus far indicates that the majority of HME systems have one or both of these characteristics, particularly given that solid solubility is often desirable from a performance viewpoint.

In this study, we examine one such system in order to develop novel characterisation methods for a suitably 'difficult' HME dispersion. More specifically, we describe the combined use of conventional and fast DSC, heat capacity measurements by modulated temperature DSC (MTDSC), scanning electron microscopy (SEM) and solid state proton nuclear magnetic resonance (NMR) relaxometry to identify the physical state of the drug in the HME formulations while also minimising sample preparation, thereby negating artefact generation via further processing. The polymer matrix used was Eudragit® E PO, which is a methacrylate copolymer, and the poorly water-soluble model drug was felodipine, a calcium channel blocker. Felodipine and Eudragit® E PO have almost identical glass transition temperatures of approximately 45°C. Formulations with different polymer:drug ratios were investigated using SEM and a range of thermal methods to identify and quantify phase separation, while we report the use of NMR relaxometry as a means of not only identifying phase separation but also assessing domain size by measuring the spin-lattice relaxation in the laboratory (T_1) and rotating ($T_{1\rho}$) frames (19–21). In this way we intend to not only identify phase separation but also to provide novel means of quantifying and characterising the distribution of the separated domains.

MATERIALS AND METHODS

Materials and Hot Melt Extrusion

Crystalline felodipine (mp: 145°C) and the amorphous polymer Eudragit® E PO were supplied from Zhejiang Yiyuan, China and Evonik Röhm GmbH&Co.KG, Darmstadt, Germany, respectively. The amorphous felodipine was prepared by melt-cooling crystalline felodipine in a DSC pan. Hot-melt extrusion was carried out using a co-rotating twin screw Haake Minilab extruder (Thermo Fisher, Karlsruhe, Germany) with a 2 mm orifice die. For the samples containing Eudragit® E PO and felodipine the temperature was set at 160°C and the screw speed at 100 rpm, and the mixture was manually fed into the extruder.

The samples were pressed through a single orifice die, collected on a cooled conveyer belt as strands. The torque was as follows: for 10% (w/w) felodipine 23 Ncm, for 20% (w/w) felodipine 26 Ncm, for 30% (w/w) felodipine 24 Ncm, for 50% (w/w) 22 Ncm and for 70% (w/w) felodipine 20 Ncm. The fresh samples were tested using MTDSC within 10 min after the extrusion process to check for the presence of any crystalline drug. SEM and NMR relaxometry have longer sample preparation time compared to DSC; hence, there was a risk of crystallisation occurring during sample preparation. The fresh samples were therefore not tested using SEM and NMR relaxometry. The aged samples were characterised after 2 months storage at 20°C/40%RH.

Thermogravimetric Analysis (TGA)

TGA analysis was used in this study to estimate the moisture content in the hot-melt extruded formulations. TGA 2900 (TA instrument, Newcastle, USA) was used to perform all measurements. The samples were tested at 10°C/min from 25 to 280°C. The moisture contents of the HME formulations varied between 0.12% and 0.3% w/w.

Standard and Fast Differential Scanning Calorimetry (DSC)

The standard and fast DSC experiments were carried out using Q-1000 MDSC (TA Instrument, Newcastle, USA) at a heating rate of 10 and 100°C/min from −20 to 160°C, respectively. Indium and n-octadecane were used as the calibration standards for the cell constant and temperature calibrations. The onset temperatures of the melting of the calibrants were within 0.5°C of the expected values. A nitrogen purge at a flow rate of 50 ml/min was used. TA standard crimped pans were used for all measurements.

Modulated Temperature Differential Scanning Calorimetry (MTDSC)

MTDSC measurements were performed using a Q-1000 MDSC (TA Instruments, Newcastle, USA). The instrument was calibrated using a series of standards prior to measurements. Pre-dried aluminium oxide was used for heat capacity calibration. The modulation parameters used were ±0.318°C/60 sec at 2°C/min underlying heating rate. TA standard crimped pans were used for all measurements. Due to the cylindrical shape of the hot-melt extruded samples, it's often difficult to achieve good thermal contact between the sample and pan. In order to establish the degree of the effect that sample shape had on the accuracy of the measurements, the hot-melt extruded samples were tested within the glass transition region (−10°C and 90°C) repeatedly (heating-cooling-reheating).

All the hot-melt extruded samples were then heated, cooled and reheated between −10 and 160°C. The changes in the reversing heat capacity values in the T_g region during the heating and cooling cycles were analysed and used as an indicator of potential phase separation, as discussed in the subsequent section.

Scanning Electron Microscopy (SEM)

The surface and cross-section morphological features of the aged extrudates with different drug loadings were observed using SEM. Samples were sputter-coated with Au/Pd and examined using a Phillips XL20 SEM (Phillips Electron Optics, Netherlands).

Solid-State NMR Relaxometry

All NMR data were collected on a Bruker NMR spectrometer operating at 300 MHz for ^{1}H using a 4 mm double-resonance MAS probe. T_1 measurements were made by using the saturation recovery pulse sequence. A series of 256 exponentially spaced recovery times, after the initial saturating train of pulses, were used to optimise the data acquisition. Saturation recovery curves for each free induction decay (FID) were extracted from the ^{1}H NMR FID by taking the intensity of the first data point in the FID. Data analysis was carried out by non-linear least-squares fitting using the Levenburg-Marquardt algorithm and by grid-search methods. Typical 90° pulse lengths were 4 microseconds, and for $T_{1\rho}$ measurements the spin locking field was 78 kHz

RESULTS

The experimental work described below falls into three groupings. First, we characterise the raw materials, physical mixes and heat-cooled solid dispersions in terms of miscibility. Second, we characterise fresh and aged HME formulations using microscopic and thermal methods. Finally, we study the aged HME systems using NMR relaxometry. In the subsequent discussion section, we describe how the information from miscibility studies may be related to the structure and stability of the HME systems.

Thermal Characterisation of Raw Materials, Physical Mixtures and Heat-Cooled Solid Dispersions of Felodipine and Eudragit® E PO

Modulated Temperature and Conventional DSC of Raw Materials and Physical Mixes

Fig. 1 shows the reversing heat capacity (C_p) signals of the T_g region of amorphous felodipine and Eudragit® E PO

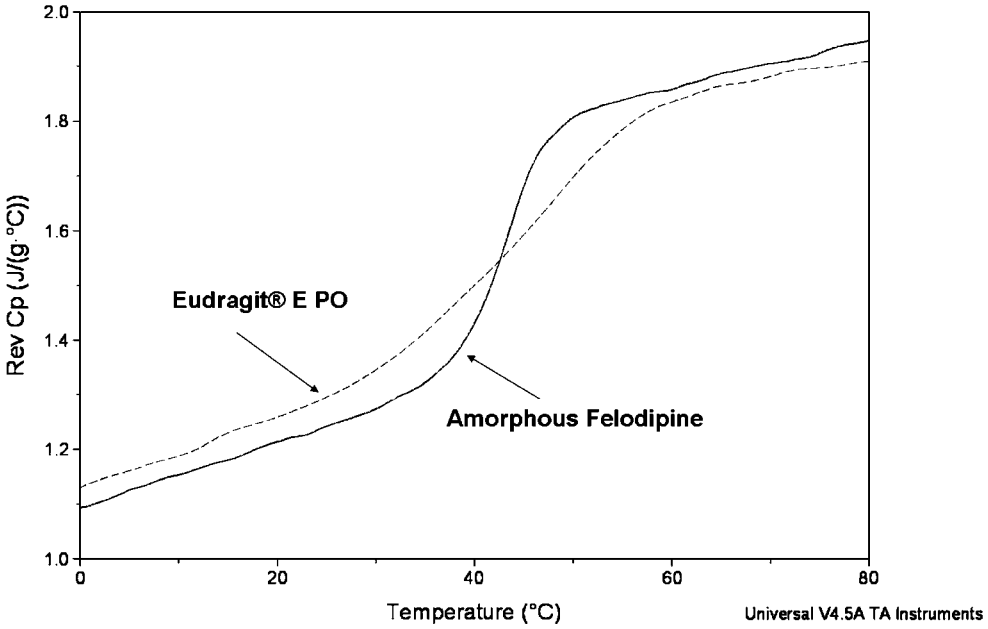

Fig. 1 MTDSC reversing C_p signals of pure Eudragit® E PO and amorphous felodipine.

alone obtained using MTDSC. It is can be seen that both materials have extremely similar T_g values (midpoint values are 43.8°C and 46.3°C for the drug and polymer, respectively). The corresponding heat capacity changes through the transition were measured as 0.479 J/g°C and 0.455 J/g°C (drug and polymer).

Physical mixtures of felodipine and Eudragit® E PO were then studied for two principal reasons. First, the melting enthalpy values of the crystalline felodipine in the physical mixtures were measured and used to produce a calibration curve to calculate the percentage drug crystallinity in the hot-melt extruded formulations. Second, we use this data to suggest a novel mathematical model whereby we are able to interpret the concentration dependence of the response in terms of the drug-polymer miscibility.

As shown in Fig. 2a, no significant depression of the melting temperature of felodipine can be seen on heating the physical mixes. Melting point depression has been used as an indication of miscibility of polymer-polymer and polymer-drug systems and to calculate the interaction parameter of the mixed systems (22–24). Although it is known that the melting point depression is heating-rate dependent (22,24), the absence of depression of the melting point of felodipine at 10°C/min may indicate low miscibility of the drug and the polymer. It also can be seen that, as expected, the ΔC_p at the polymer T_g decreases on lowering the percentage of polymer in the mix as the crystalline drug does not contribute to the C_p change prior to its melting transition.

The enthalpy values of the endothermic peaks of the physical mixes were then calculated and plotted against the weight fraction of felodipine in each mixture (Fig. 2b) in order to gain insight into the solubility of felodipine in Eudragit® E PO during melting. The x-intercept of the curve has been previously interpreted as representing the solubility of the API in the polymer at a specific heating rate (25,26). However, we wish to reconsider the significance of the curve intercept as follows. The enthalpy value of the endothermic peak may be considered to represent the energy involved in the drug dissolution in the softened ($>T_g$) polymer in combination with the melting of the crystalline drug; one may consider both processes to occur to some extent simultaneously, or, alternatively, depending on loading, one or the other may predominate. For high drug concentration systems (50%, 70% and 90% w/w), the polymer is no longer in great excess, and some polymer may start to dissolve in the molten drug instead of *vice versa*, hence adding a third possible process that may occur during the endothermic event.

It is convenient to assume that on melting initially a two phase system is formed with a polymer-rich phase (Phase 1: drug dissolved in polymer) and a drug-rich phase (Phase 2: polymer dissolved in molten drug). In practice, the amounts of one substance dissolved in another may be very small but will be finite and will, for the time being, be considered as significant to the model.

The solubility (expressed as mass ratio) of the drug in the polymer (K_D) is defined by

$$K_D = M_{D1}/M_{P1} \quad (1)$$

where M_{D1} is the mass of the drug dissolved in Phase 1 and M_{P1} is the mass of the polymer in Phase 1. Similarly, the solubility of the polymer in the molten drug (K_P) can be expressed by

$$K_P = M_{P2}/M_{D2} \quad (2)$$

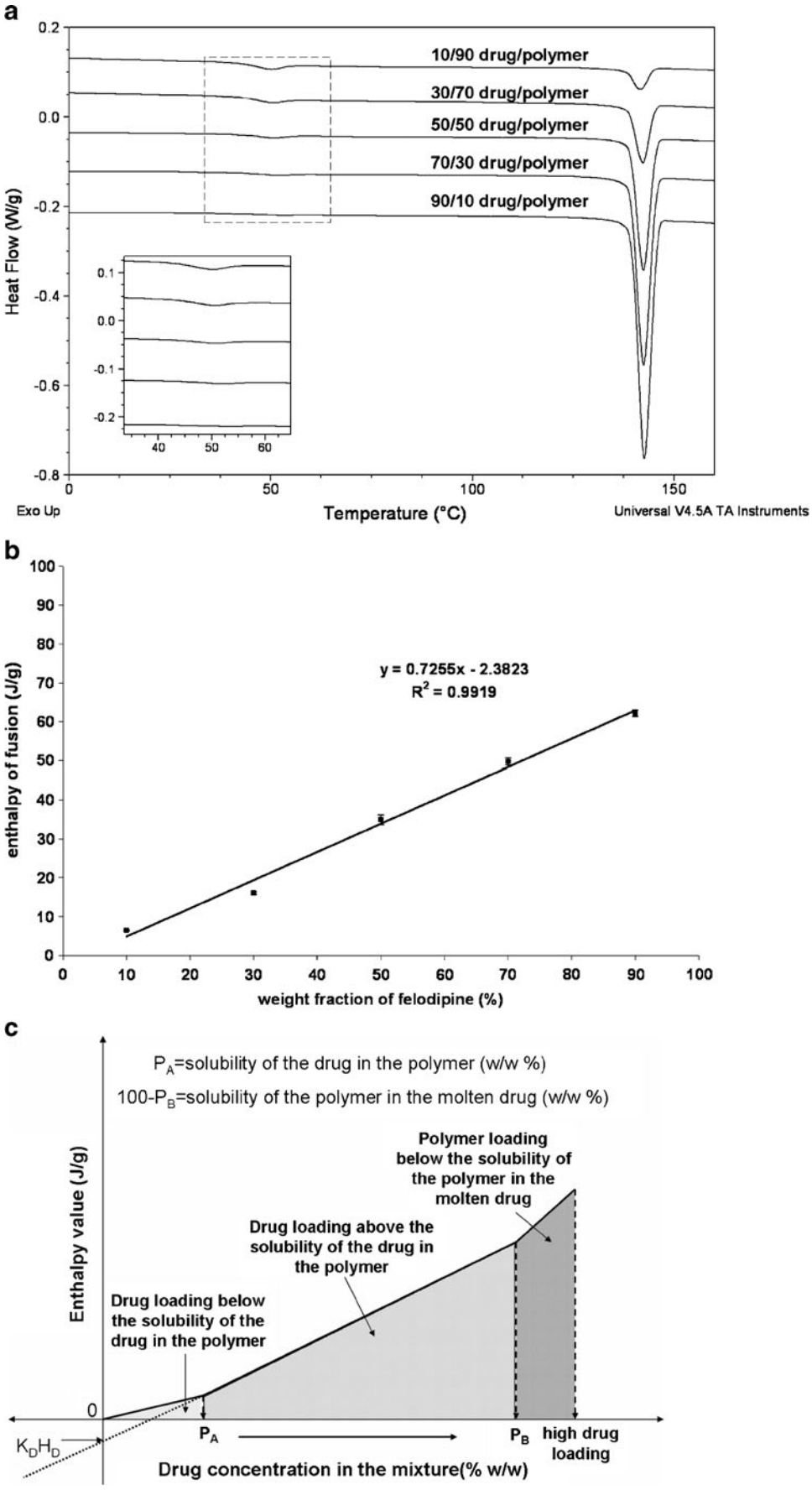

Fig. 2 **a** Conventional DSC (heating at 10°C/min) responses of physical mixtures of Eudragit® E PO and felodipine with insert view of T_g region. **b** Calibration plot of the percentage (w/w %) of crystalline felodipine against the enthalpy values of the endothermic transitions of the physical mixtures of Eudragit® E PO and felodipine (error bars represent the range for $n = 3$ measurements). **c** Illustration of enthalpy-drug concetration plot for the physical mixes with full range of drug/polymer ratios.

where M_{D2} is the mass of the drug dissolved in Phase 2 and M_{P2} is the mass of the polymer dissolved in Phase 2. The mass balance is given by $M_D = M_{D1} + M_{D2}$ and $M_P = M_{P1} + M_{P2}$, where the total mass is $M_D + M_P$. If in Phase 1 the enthalpy of dissolution of the drug in the polymer is H_D, and in Phase 2 the enthalpy of dissolution of the polymer in the molten drug is H_P, using Eqs. 1 and 2 we can write:

$$H_t = H_f M_D + K_D M_{P1} H_D + K_P M_{D2} H_P \tag{3}$$

where H_t is the total amount of heat change of the endothermic peak and H_f is the heat of fusion of the drug. Since no melting point depression was observed, it is reasonable to predict that the drug and polymer have low miscibility. If the solubility of the drug in the polymer (K_D) and the solubility of the polymer in the molten drug (K_P) are small, then we may approximate $M_{P1} = M_P$ and $M_{D2} = M_D$. If the weight fraction of drug and polymer in the whole mixture are given by X_D and X_P, and the approximation above stands, then

$$\begin{aligned} H_t/(M_D + M_P) &= H_f X_D + K_D H_D (1 - X_D) + K_P H_P X_D \\ &= X_D\left(H_f - K_D H_D + K_P H_P\right) + K_D H_D \end{aligned} \tag{4}$$

This gives a linear expression of heat of fusion against composition, with the y-intercept predicted as $K_D H_D$. It should be noted that the heat of dissolution of the drug in the polymer H_D may be reasonably expected to be exothermic due to bond formation between the polymer and drug (27). This in turn will lead to the observed finite value of concentration at zero enthalpy (the x-axis intercept); our argument is that rather than indicating the value of drug solubility in the polymer, this is in fact a composite value that represents both the solubility and the heat of dissolution. It is not possible at this stage to deconvolute these two parameters, but it is nevertheless helpful to have a theoretical basis for interpreting the x-axis intercept.

Two further, more extreme situations may be considered. If the drug loading is considerably lower than the solubility of the drug in the polymer, i.e. only Phase 1 is present, then the Eq. 4 can be modified by incorporating Eqs. 1 and 3 as

$$H_t/(M_D + M_P) = X_D\left(H_f + H_D\right) \tag{5}$$

In Eq. 5, it is clear that the linear relation crosses the origin with a zero value of the x-intercept. At the other extreme of high drug loading systems, if the amount of polymer is lower than the solubility of the polymer in the molten drug, i.e. only Phase 2 present, then Eq. 4 can be modified by incorporating Eqs. 2 and 3 such that

$$H_t/(M_D + M_P) = X_D\left(H_f - H_P\right) + H_P \tag{6}$$

Ideally, if the physical mixture with all drug concentrations is examined and the enthalpy values are plotted, one should expect to see three regions of behaviour as demonstrated in Fig. 2c. These include a low drug concentration region where the drug loading is lower than the drug solubility in the polymer presented by Eq. 5, an intermediate drug concentration region which obeys Eq. 4, and a high drug concentration region where the drug loading is higher than the polymer solubility in the molten drug expressed by Eq. 6. At low drug concentration a linear region exists where the slope is ($H_f + H_D$) with a zero intercept. Thus theoretically we could extract H_D using the slope of the low concentration linear relation since H_f is experimentally measurable. Then the H_D value is substituted into Eq. 4 (modified form for the presence of Phase 1 only) to calculate K_D. Similarly at very high concentrations of drug we could find H_P using the slope or x-intercept and in principle extract K_P. However, the heat change at each extreme can be very low so the accurate measurement experimentally can be very difficult to achieve. The drug solubility in the polymer is at the concentration where the straight lines of the low and intermediate drug concentration regions join (point P_A). In the case reported here, no indication of a break in the line is observed suggesting that the concentration range studied is within the intermediate region presented in Fig. 2c. The lowest felodipine concentration used in the linear correlation is 10%, therefore it is reasonable to predict that the solubility of felodipine in Eudragit® E PO is around 10% when tested using 10°C/min heating rate. Since this method estimates the drug solubility in polymer at the melting temperature of the drug, the true drug solubility in polymer at storage temperature (higly associated with the physical stability of the formulation) is likely to be lower than the estimated value. The significance of this prediction will be discussed later.

Modulated Temperature DSC (MTDSC) of Heat-Cooled Systems

MTDSC was used to study the thermal events associated with the cooling and re-melting processes of the physical mixtures. The principle of MTDSC is that a perturbation (typically, but by no means exclusively, a sine wave) is superimposed on the underlying heating signal such that the response may be considered in terms of both the response to the sine wave and the underlying signal, thereby adding a further source of data compared to conventional DSC. The total heat flow may be described by

$$dQ/dt = C_p.dT/dt + f(t, T) \tag{7}$$

where Q is the heat evolved, C_p is the heat capacity (the energy stored in molecular motions available to the sample)

and $f(t,T)$ is a function of time and temperature that governs the kinetically hindered response associated with physical or chemical changes (28). Deconvolution of the response is usually performed by a simple analysis whereby the heat capacity is calculated via

$$C_p = K_{CP}\left(A^{MHF}/A^{MHR}\right) \tag{8}$$

where K_{cp} is a heat capacity calibration constant, A^{MHF} is the amplitude of the modulated heat flow and A^{MHR} is the amplitude of the modulated heating rate; this then gives the first term on the right side of Eq. 7, which is known as the reversing heat flow signal as it refers to energy that is entirely dependent on the sample temperature. By subtracting the calculated heat capacity from the underlying heat flow, it is possible to obtain $f(t,T)$, which yields the non-reversing heat flow, reflecting kinetically hindered events such as crystallisation. It is also possible to perform a more sophisticated deconvolution whereby the phase angle (θ) between the heat flow response and the modulated heating rate is taken into account (hence bearing a greater resemblance to the deconvolution of dielectric or oscillatory data); in this case the heat capacity is considered to be a complex number whereby

$$C_p' = C_p^* \cos\theta \tag{9}$$

and

$$C_p'' = C_p^* \sin\theta \tag{10}$$

The real component (C_p') arises from reversing processes and is in phase with the modulation, while the imaginary component (C_p'') reflects kinetic processes and is out of phase with the modulation. In a practical sense, the values of the phase lag tend to be small except through melting processes, and hence C_p' and C_p^* tend to be very similar; hence, in most applications the simple deconvolution process is satisfactory (28).

Solid dispersions of felodipine and Eudragit® E PO were prepared by a fusion method whereby physical mixtures of felodipine and Eudragit® E PO were heated to 160°C, then cooled at 10°C/min. Fig. 3 shows the reversing C_p signals of cooling (160–0°C) and reheating (0–160°C) of the physical mixtures after the first melting seen in Fig. 2a. There are no exothermic/endothermic transitions observed during cooling-reheating in all samples, indicating the absence of crystalline drug within the systems. It is interesting to note that the freshly prepared hot-melt extruded samples with drug loading from 10% to 50% showed the same thermal behaviour except 70% drug loading, which showed a melting transition at 129°C.

The measured T_g values (taken at the midpoint of the transition) were also very similar for all solid dispersions formed from the physical mixes. Given the similarity of the T_g values of the raw materials, it is difficult to ascertain for certain whether the system is phase separated or otherwise, although the symmetry of the transition and the absence of any indication of two glass transitions would suggest miscibility. Similarly, since the C_p values of the amorphous drug and polymer are very close, it is difficult to assess miscibility by looking at the relationship between C_p and composition. Since the solid solubility of felodipine in Eudragit® E PO has been predicted as being around or below 10% w/w, it is reasonable to suggest that the physical mixture with 10% felodipine may form a one-

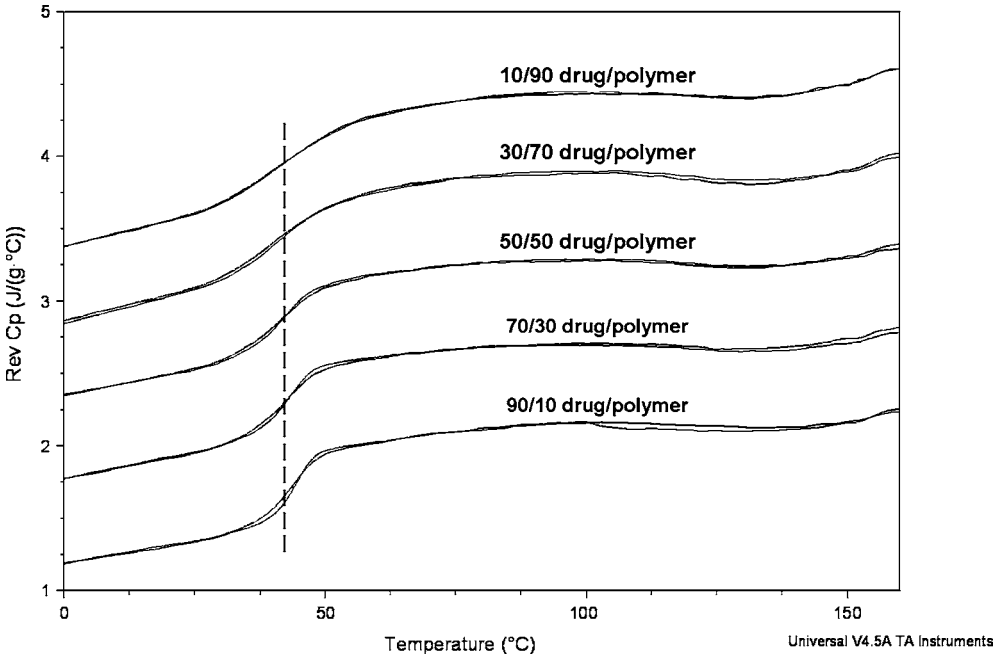

Fig. 3 MTDSC reversing C_p signals of the solid dispersions of Eudragit® E PO and felodipine prepared by fusion of the polymer and the crystalline drug during cooling and reheating.

phase system. For the systems with drug loading above 10%, the cooling-reheating reversing signals of each individual system are effectively superimposible with the absence of exothermic/endothermic transitions, indicating two possibilities: either the formations of a two-phase system with separate amorphous domains or else a supersaturated one-phase system. In either case, the systems are expected to show physical instability over storage.

It is noted that despite a theoretical solubility of ≤10% w/w felodipine within the polymer, no crystalline drug is found in the solid dispersions with drug loading up to 90% w/w prepared by fusion, while drug crystallisation is evidenced in the fresh HME systems with drug loading above 50% w/w. This deviation between the solid dispersions prepared by fusion and HME is possibly a result of the different physical stresses of the samples experienced during preparation. In the hot-melt extruder, the samples went through multiple physical stresses, such as high sheer, high pressure and high temperature; whereas the samples prepared by fusion only experienced the temperature stress. Although the mechanism of how the physical stresses during hot-melt extrusion can influence the solidification behaviour of the post-extrusion sample is not entirely clear, similar phenomena have been observed in other solid dispersion systems prepared by other manufacturing processes, such as spray drying and film casting. This will be further explored in a future study.

Thermal and Microscopic Analysis of Aged HME Systems

SEM Analysis of Aged HME Formulations

In this section, the structure and miscibility of the drug within the HME systems stored for 2 months were examined. In the first instance, SEM was used to ascertain whether there was any evidence for phase separation in the extrudates. A recent study has shown the uneven spatial distribution of crystalline drugs in HME cylinder-shaped extrudates (18). The cause of the uneven distribution of drug crystals is likely to be associated with the expansion process of the sample immediately after extrusion. The expansion process may further generate a drug concentration gradient across the extrudate which may have impact on the crystallisation behaviour of the drug during aging. Both the surfaces and cross-sections of the HME systems were analysed. As seen in Fig. 4, the surface and cross-section of the aged HME extrudate with 10% drug loading were smooth with no visible drug crystals. In the case of the aged extrudates with 20% drug loading, the surface of the cylinder was uniform with no drug crystals observed; however, a few small granules scattered on the cross-section of the 20% system were visible. The SEM images of the surface of the aged HME extrudates with 30% drug loading showed the presence of a significant amount of

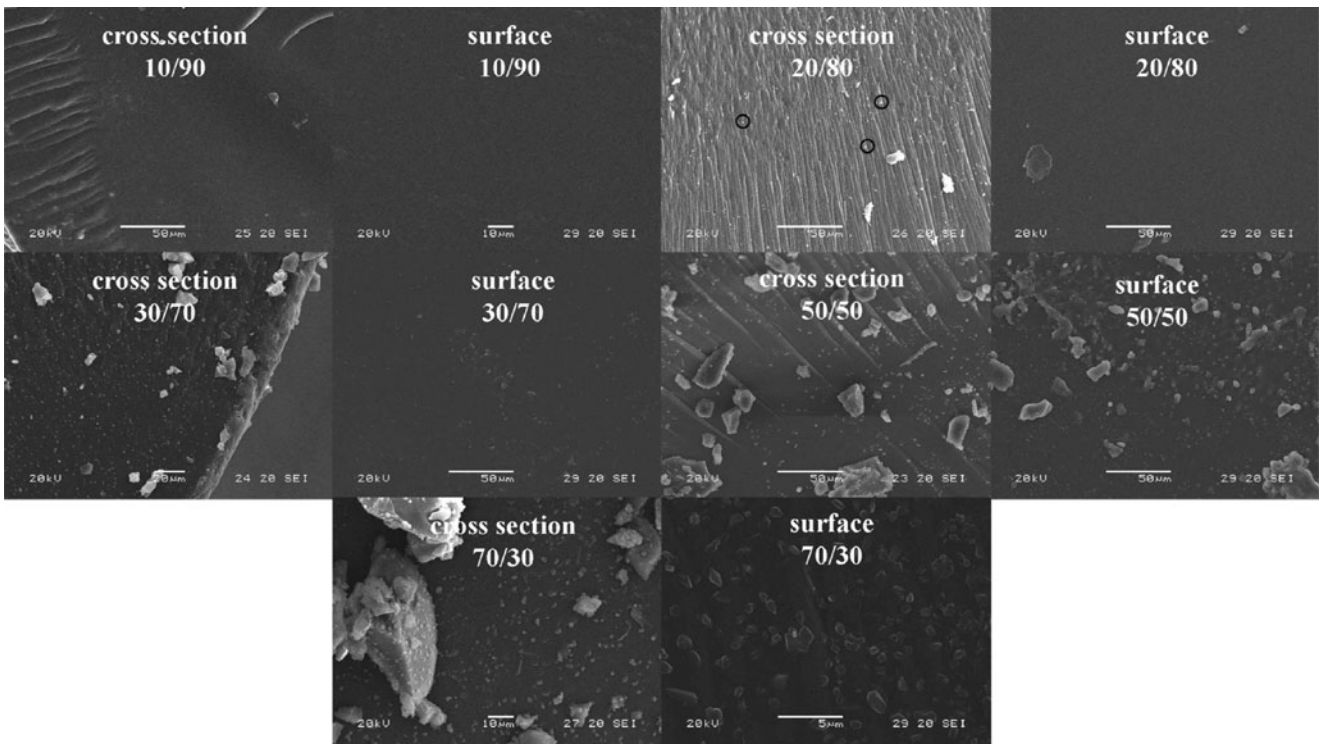

Fig. 4 SEM images of the cross-sections and surfaces of the aged HME formulations with different drug loadings.

granules with dimensions of approximately 1 micron; more granules were seen on the cross-section than on the surface of these extrudates (Fig. 4). The surface and the cross-section images of the aged HME extrudates with 50% and 70% drug loading all similarly showed the appearance of the granules, with the density of the white granules increasing with increased drug loading. As seen in the SEM image of the surface of the 70% system (Fig. 4), the granules were between 1–3 micron in diameter with defined edges.

There is therefore compelling evidence for the presence of phase separation within the aged HME formulations. We note that while there has been considerable attention extended to the detection of small amounts of amorphous material in otherwise crystalline materials, the same is not true in reverse. On that basis, we explore the quantification of small quantities of crystalline material using a novel thermal approach in the subsequent sections.

Conventional and Fast DSC Studies of Aged HME Formulations

Fig. 5 shows the conventional DSC results of the aged HME formulations studied at a heating rate of 10°C/min. It can be seen that all five formulations have a clear single glass transition. The aged HME formulation with 10% drug loading shows a marked relaxation endotherm at the glass transition which is a result of the presence of a large proportion of the polymer since the polymer alone showed a strong relaxation peak at T_g (data not shown). The aged formulation with 70% drug loading showed a melting transition at a temperature of 136.7°C, which corresponds to the melting temperature of felodipine polymorphic form II reported previously (29–32), whereby it has been suggested that glassy felodipine is likely to recrystallise into different pseudo and metastable polymorphic forms including form II. However, one could also argue that this lower melting point could reflect melting point depression of the drug by the polymer as it is well known that the melting point of the API can be depressed in solid dispersion formulations due to the miscibility between polymer and drug (22,23,33). We believe that this is unlikely to be the case here as no melting point depression was observed in the physical mixes of the drug. Fast DSC was also used to examine all aged samples, since the high scanning rate may reduce the dissolution effect of crystalline material in the polymer during heating. However, the fast DSC results for all aged HME formulations were identical to the conventional DSC results (data not shown). This indicates that either there is no crystalline in the 10–50% drug-loaded formulations or the heating rate applied in this study is not effective enough to overcome the dissolution of the crystalline drug in the glassy polymer.

Modulated Temperature DSC Studies of Aged HME Formulations

The above data support the SEM studies in suggesting that there is crystalline material present in the aged HME formulations, at least in the 70% w/w systems. The observation that no clear melting was observed in the lower drug content systems leads to three possible explanations. First, the formulations with drug loadings from 10–50% could be one-phase systems (solid solutions). Second, the formulations may have phase separated into two amorphous

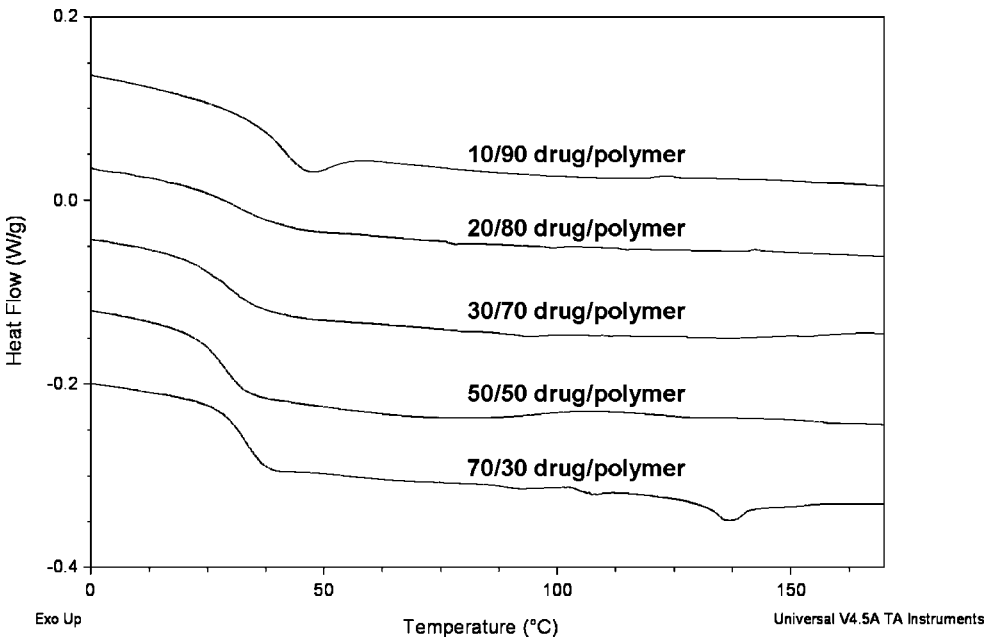

Fig. 5 Conventional DSC (heating at 10°C/min) responses of the aged HME formulations.

materials, this typically being considered to be the stage before drug recrystallisation. However, as discussed previously, in this case it is difficult to confirm the phase separation using T_g measurements. Finally, the formulations are phase separated with crystalline drug. However, due to their low quantity and small size, the crystals of the drug dissolved into the glassy polymer prior to melting and hence are not detected.

Given the SEM and DSC evidence for the presence of crystallites, along with the paucity of techniques available for the detection of small quantities of crystalline material, we explore the third explanation in more detail. We suggest that, although no clear melting can be seen for the aged 10–50% w/w samples, if crystallites are present, the reversing C_p signal should still show changes after first melting, since crystalline material can contribute to a lower total C_p compared to their pure amorphous phase at temperatures above T_g. This is because the increase in heat capacity of an amorphous material going through its T_g is caused by the changes in molecular vibration and configurational entropy. More specifically, at temperatures below T_g, the C_p is close to that of the crystalline form, but on heating through T_g, intermolecular potential energy that depends on the relative orientation of the molecules and the segments within the molecule contributes to the C_p (34). Therefore, the C_p value of an amorphous material is significantly higher than its crystalline form at temperatures above T_g. It follows that by heating to 160°C the drug crystals will melt and dissolve in the polymer, thereby contributing to an increase in C_p which will be seen on cooling. The difference in C_p between the first heating and cooling cycles is therefore a direct reflection of the presence of crystallites within the sample and could, we suggest, provide a novel means of quantifying such material. We propose a model below to address this issue. However, in order to develop this approach it is essential to be able to make accurate C_p measurements, and this in turn necessitates careful consideration of the sample presentation to the DSC; this is considered below.

As discussed in the Methods section, due to the unique cylindrical shape of the HME extrudates, good thermal contact between the sample and pan may be difficult to achieve; this may lead to poor data acquisition and unreliable C_p estimation. Therefore, it is important to first establish the reliability of the direct measurements on the HME strands using MTDSC. This can be achieved by assessing the T_g region (0–90°C) repeatedly using heating-cooling cycles and measuring the variation of the T_g and ΔC_p value during the cycles. The lack of significant changes in the values of the two parameters can be a good indicator of satisfactory thermal contact between the sample and the DSC pan, as heating beyond T_g is expected to facilitate sample flow which may potentially alter the measurements if contact was initially poor. As seen in Fig. 6, the T_g and ΔC_p values of the heating-cooling cycles are superimposeable. This indicates that the shape of extrudates does not significantly affect the accuracy of the measurements.

The aged HME extrudates were then tested using the same heating-cooling cycles (0–160°C) applied to the solid dispersions prepared by fusion. All formulations showed significant increases in the reversing C_p value in the cooling and the second heating compared to the first heating, while no clear melting of crystalline form felodipine was observed during the first heating except the aged 70% drug-loaded system; the dashed areas are the differences between the first heating and cooling (Fig. 7). The reversing C_p signal of the cooling process almost superimpose with the reheating signal, indicating that the changes are irreversible. As mentioned previously, since the C_p of the amorphous felodipine and Eudragit® E PO is very similar, one should expect no changes during heat-cool if the formulations are one-phase or phase separated with amorphous drug domains. In contrast, if the phase-separated system contains crystalline felodipine, the reversing C_p values of the first heating of the samples should be lower than the cooling and reheating since the C_p value of crystalline drug is lower than the amorphous drug at temperatures above its T_g. It is known from the study on the freshly prepared solid dispersions of felodipine and Eudragit® E PO that supersaturated system can be formed, and no immediate crystallisation observed; hence, it is reasonable to suggest that if crystalline material is indeed present, the C_p values show increase on cooling compared to the initial heating run. Inspection of Fig. 7 clearly shows this to be the case.

From the changes observed in C_p during heating and cooling, it is possible to calculate the amount of crystalline drug present in the original aged samples using an adaptation of the method described by Xu *et al.* for calculating the quantity of rigid amorphous fraction in polymers (35). The total heat capacity of the sample can be expressed as

$$C_p^{total}(T) = \phi C_p^{drug}(T) + (1-\phi) C_p^{polymer}(T) \tag{11}$$

while the heat capacity contribution of the drug may be expressed as

$$C_p^{drug}(T) = x C_p^{amorphous}(T) + (1-x) C_p^{crystalline}(T) \tag{12}$$

where $C_p^{total}, C_p^{drug}, C_p^{polymer}$ are the total heat capacity, the heat capacities of drug and the polymer, respectively, at temperature T, and $C_p^{amorphous}$ and $C_p^{crystalline}$ are the heat capacities of amorphous and crystalline drug at temperature T; ϕ is the weight fraction of the drug in the extrudate and x is the weight fraction of amorphous drug in the total

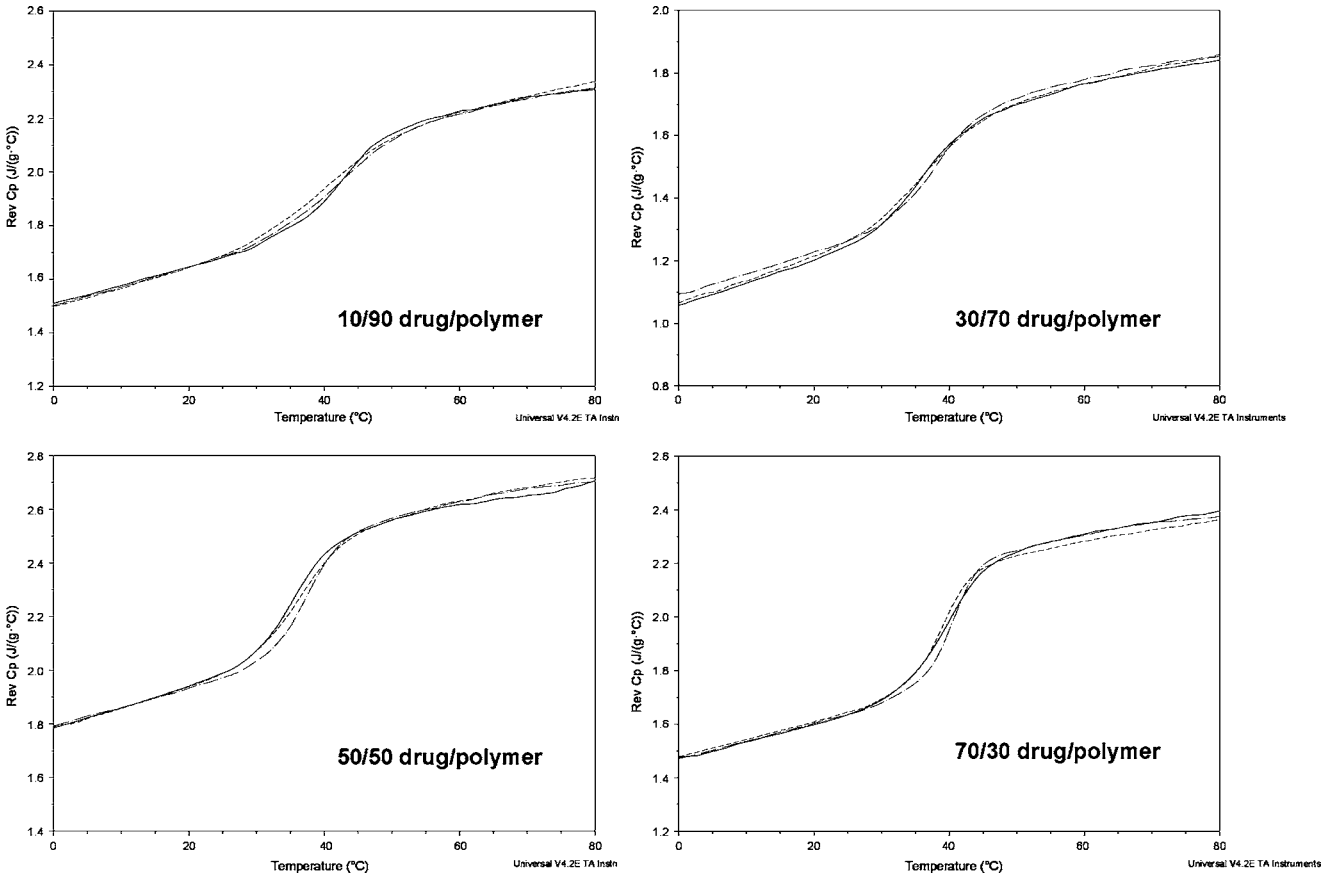

Fig. 6 MTDSC reversing C_p signals of the aged HME formulations in the course of heating, cooling and reheating between −10 to 90°C at 2°C/min (T_g region). (*Solid line* is first heating, *long dash* is cooling and *short dash* is the reheating).

amount of drug present in the extrudate. By combining Eqs. 11 and 12, the total heat capacity of the system can be expressed using Eq. 13:

$$C_p^{total}(T) = \phi\left[xC_p^{amorphous}(T) + (1-x)C_p^{crystalline}(T)\right] + (1-\phi)C_p^{polymer}(T) \quad (13)$$

After the first heating to 160°C, any crystalline drug will be melted. Therefore, it is reasonable to assume that all felodipine is in amorphous state during cooling. The total heat capacity of the cooling stage can then be expressed as

$$C_p^{total}(T) = \phi C_p^{amorphous}(T) + (1-\phi)C_p^{polymer}(T) \quad (14)$$

Therefore, the change in total heat capacity, $\Delta C_p^{heat-cool}$ at temperature T, between first heating and cooling can be expressed using Eq. 14 minus Eq. 13:

$$\Delta C_p^{heat-cool}(T) = \phi(1-x)\left(C_p^{amorphous}(T) - C_p^{crystalline}(T)\right) \quad (15)$$

The $\Delta C_p^{heat-cool}$, $C_p^{amorphous}$ and $C_p^{crystalline}$ at temperature T (which is 80°C for this study) can be measured by MTDSC experiments as seen in Fig. 7, while ϕ is the known drug loading of the formulation. Therefore, the fraction of amorphous and crystalline drug in the aged formulations can be calculated.

The calculated crystalline drug contents are 60.1% w/w, 34.1% w/w, and 14.3% w/w for the aged 10%, 30% and 50% (w/w) drug-loaded formulations, respectively; these figures reflect the proportion of the total drug present, not the total sample; hence, the values for the proportion of the sample as a whole that is crystalline drug may be calculated as 6.01%, 10.23% and 7.15%. These values are all of the same order of magnitude and indicate that on storing for 2 months a significant proportion of the drug separates as crystals, despite there being no evidence for the presence of crystallites in the freshly prepared heat-cooled samples of the freshly prepared HME systems. The possible cause of 30% drug-loaded formulation containing the higher crystalline drug than the 50% drug-loaded formulation is that the difference in the degree of supersaturation leads to the different nucleation and crystallisation pathways of the two formulations. This hypothesis will be tested experimentally in a separate study.

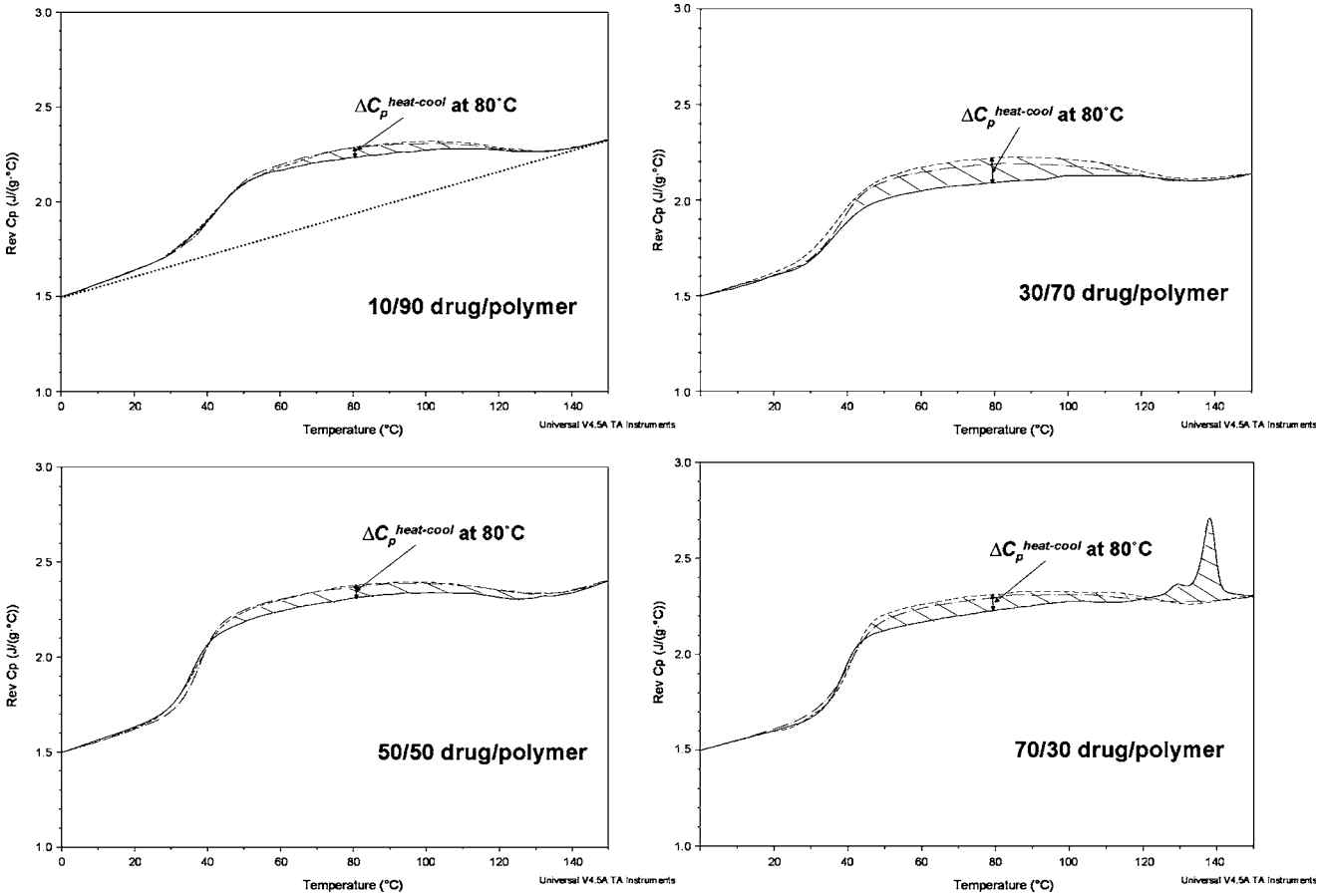

Fig. 7 MTDSC reversing C_p signals of the aged HME formulations with drug loadings 10–70% in the course of heating, cooling and reheating between −10 to 160°C at 2°C/min (*Solid line* is first heating, *short dash line* is cooling and *dash dot line* is the reheating).

Proton-NMR Relaxometry Studies of the Aged HME Formulations

Proton-NMR relaxometry is a powerful technique for detecting phase separation with sub-micron dimensions (19–21). In this study, proton NMR relaxometry was used to confirm the presence of phase separation detected using SEM and heat capacity measurements. The ^{1}H spin lattice relaxation times of the HME formulations, T_1, and the spin-lattice relaxation times in the rotating frame, $T_{1\rho}$ are summarised in Table I. It can be seen that only one T_1 relaxation time was detected for the aged HME formulations with 10% and 20% drug loading, whereas two components are seen for the aged systems with 30%, 50% and 70% drug loading, one with a long relaxation time (around 1 s) and the other relaxation time is shorter (around 0.5 s). It is noted that for all three formulations (with 30%, 50%, and 70% w/w drug loading), the two components of the T_1 relaxation times are very similar. Taking into account the amplitude of the two components

Table I ^{1}H T_1 Spin-lattice Relaxation Time and $T_{1\rho}$ Spin-lattice Relaxation Time in the Rotating Frame of the Aged HME Formulations Measured at 300 MHz

Drug/polymer ratio	10:90	20:80	30:70	50:50	70:30
T_1 amplitude	1.00	1.00	0.67	0.49	0.43
	0.00	0.00	0.33	0.51	0.57
T_1 time constant (s)	0.59	0.60	0.55	0.54	0.58
	0.00	0.00	0.99	0.95	1.06
$T_{1\rho}$ amplitude	0.84	0.85	0.67	0.75	0.24
	0.16	0.15	0.33	0.25	0.76
$T_{1\rho}$ time constant (ms)	1.05E-03	1.16E-03	2.62E-03	1.28E-03	2.70E-03
	1.34E-02	1.30E-02	1.32E-02	1.19E-02	1.96E-02

in the T_1 relaxation times of these three formulations, it is reasonable to suggest that the short relaxation time components are associated with phase separated felodipine. However, it is difficult to identify felodipine as being in crystalline or amorphous form, since it is likely that the two relaxation times would be similar at room temperature (29). The percentage of the slow decay component increases with drug loading. It has been confirmed by DSC that crystalline felodipine is present in the aged extrudates with 70% drug loading. Therefore, it is reasonable to conclude that the shorter relaxation time is related to the presence of crystalline felodipine, and thus there are crystalline domains in the aged formulations with 30% and 50% drug loading. Taking into account the absence of melting transitions in the DSC results of the aged 30% and 50% formulations, it is likely the dimensions and the quantity of the felodipine domains in these two formulations are smaller than the ones in the aged formulation with 70% drug loading, which leads to the fast dissolution of sub-micron crystals during heating. Although the aged formulations with 10% and 20% drug loading appear as a single phase in the T_1 measurements, the $T_{1\rho}$ measurements reveal two components in these formulations (Table I). This is likely to be caused by the difference in the time scales of T_1 and $T_{1\rho}$. If the phase-separated domain size is smaller than the diffusive path length within the T_1 time scale, the T_1 measurements can not separate different relaxation times for different phases, but the $T_{1\rho}$ measurements should be able to detect the separation (21).

For a heterogeneous system, the relaxation time of different phases can be further used to estimate the dimension of the separated phases (20,21). The observation of two separate relaxation processes for $T_{1\rho}$ relaxation indicates the existence of at least two separate domains which are not in the fast exchange limit. Assuming the process of exchange is by spin diffusion and not matter diffusion, the following relationship is valid (21):

$$2\sqrt{2}\left(A^2/\pi^2 D\right)|\Delta\gamma| > 1 \tag{16}$$

where A is the dimension over which diffusion takes place and is indicative of the smallest dimension of the separated domains, D is the spin-diffusion coefficient mediating exchange between the two phases, and $\Delta\gamma$ is the difference in the relaxation rates of the separated phases (21). The spin-diffusion coefficient (D) has a typical value in polymeric systems as $10^{-16}\mathrm{m}^2\mathrm{s}^{-1}$ (36). The $\Delta\gamma$ value can be calculated using Eq. 17:

$$\Delta\gamma = \frac{1}{T_A} - \frac{1}{T_B} \tag{17}$$

where T_A and T_B represent the relaxation time of phase A and phase B. The T_1 measurements revealed the phase separation in the systems with 30, 50, and 70% drug loading. However, the $T_{1\rho}$ measurements indicate that all HME formulations are heterogeneous in nature. Using Eq. 16, the size of the domains can be estimated. The average values of the long T_1 and short T_1 of the HME formulations were used to estimate the domains, sizes measured in the T_1 experiments. These values indicate that the diffusional path length of the neighbour domains has to be greater than 22 nm to be detectable. A similar calculation was carried out for the $T_{1\rho}$ experiments. The domain size was calculated as greater than 5.6 nm. This indicates that in the aged HME formulations with 10% and 20% drug loading the intimate mixing of the drug and the polymer is on scale of less than 22 nm but greater than 5.6 nm. The results can not be interpreted as the accurate size measurement of the domains, but an approximate estimation. If the phase-separated material is at low concentration and has dimensions on the nano-meter scale, MTDSC may not be sensitive enough to detect it. This is because the domains (separated phases) may dissolve into each other during heating, and the endothermic energy could be too weak to be analysed.

DISCUSSION

The main aim of this study was to address three key areas of understanding with regard to HME solid dispersion formulations. First, we wished to explore the question of basic miscibility between the drug and polymer; second, we wished to develop novel approaches to detecting phase separation (particularly for systems containing components with similar T_g values), and third, we wished to explore the correlation between the two in the sense of developing predictive models for physical stability. A successful outcome to the study would therefore lead not only to new characterisation approaches but also the basis for predicting long-term stability of HME formulations.

In the first instance, the solid solubility of felodipine and Eudragit® E PO was assessed. The absence of melting-point depression in the felodipine-Eudragit® E PO physical mixtures at 10°C/min scanning rate leads to the assumption of low solid solubility of the drug in the polymer. The enthalpy of the melting peak of each physical mixture was calculated and plotted against the percentage of crystalline drug in the mixes (Fig. 2b). It can be seen that the physical mixtures have a good linear correlation between the enthalpy values and the percentages of crystalline drug (enthalpy-drug concentration plot). A novel interpretation of the linear relationship observed was presented in terms of the decrease in enthalpy being a function of both composition and enthalpy of interaction between the drug and polymer, thereby allowing estimation of the solubility of the drug in the polymer. However, it is worth pointing out that

the heating rate used for testing the systems can affect the predictive result of this method. This effect can be significant for the systems with high solubility of one in the other. It was estimated that the solubility of felodipine in Eudragit® E PO is ≤10% w/w at the melting temperature of felodipine (tested using 10°C/min heating rate). With further study we believe that the model could be refined to allow more specific predictions but would require knowledge of the enthalpy of interaction to achieve this. Nevertheless, the approach has allowed us an insight into the likely equilibrium solubility range for this particular system.

Taking this argument to the next logical stage, we can predict that the HME formulations (and indeed heat-cooled systems) under study here have drug loadings above the predicted miscibility; hence, it is logical to suggest that such systems will not be stable on storage even if the drug appears to be initially molecularly dispersed in the polymer. However, before we are able to confirm this, it is essential to develop methods for assessing phase separation, particularly as the T_g values for the two components are very similar. We suggest three methods for assessing this separation. First, we present SEM data which indicated that there was strong evidence for the presence of crystallites; second, we present a novel method whereby heat capacity measurements on cycling may be used to calculate drug separation; and third, we use solid-state NMR relaxometry to estimate phase separation and domain size. In all three cases it was found that there was compelling evidence for extensive phase separation for the aged HME systems (circa 5–10% of the total), with the likelihood being that the drug is present as a mix of crystallites and nanoscale domains. The latter would easily explain the absence of direct thermal (melting) evidence for separation for systems containing up to 50% drug as such domains would be expected to dissipate into the polymer on melting.

This in turn leads to the third consideration, namely the potential for using these combined approaches as a means of predicting stability. Our data indicates that if one formulates above the miscibility of the drug in the polymer, it is perfectly possible to generate a single-phase system, but the likelihood appears to be that this phase will separate on storage. We also suggest that miscibility may be easily assessed by simply heating physical mixes of the drug and polymer and observing the melting behaviour. In this manner, it is intended that not only may phase separation be studied more reliably (and the shortcomings of conventional approaches such as DSC appreciated) but also that it is possible to predict long-term stability from simple early measurements.

CONCLUSION

This study describes the development of a simple physical stability prediction method for solid dispersion-based formulations and novel approaches to investigate phase separation in systems in which the drug and polymer have similar T_gs. The prediction of the solid solubility of felodipine in Eudragit® E PO was ≤10% (w/w) using the enthalpy-drug concentration plot conducted by the physical mixture study. This leads to the prediction that formulations with drug loadings at and above 10% (w/w) may have potential physical instability over aging. The experimental results of the aged HME samples confirmed that presence of phase separation in all samples, indicating the formulations with drug loading above the solid solubility of the drug have physical instability. This study also explored the use of heat capacity measurements using MTDSC combined with NMR relaxometry to overcome the difficulties of identifying phase separations in systems in which the drug and polymer have similar T_gs and dissolution of crystalline drug particles in the glassy polymer below the drug melting point. Overall, the study has provided novel approaches to assessing both miscibility and phase separation and has suggested an intimate link between the two parameters that may be used to predict physical stability.

ACKNOWLEDGEMENTS

The authors would like to thank Mr. Frederik Klama for his contribution to the NMR data collection.

REFERENCES

1. Miller DA, McConville JT, Yang W, Williams III RO, McGinity JW. Hot-melt extrusion for enhanced delivery of drug particles. J Pharm Sci. 2006;96(2):361–76.
2. Leuner C, Dressman J. Improving drug solubility for oral delivery using solid dispersions. Eur J Pharm Biopharm. 2000; 50(1):47–60.
3. Breitenbach J. Melt extrusion: from process to drug delivery technology. Eur J Pharm Biopharm. 2002;54(2):107–17.
4. Forster A, Hempenstall J, Tucker I, Rades T. Selection of excipients for melt extrusion with two poorly water-soluble drugs by solubility parameter calculation and thermal analysis. Int J Pharm. 2001;226(1–2):147–61.
5. Lalkshman JP, Cao Y, Kowalski J, Serajuddin ATM. Application of melt extrusion in the development of a physically and chemically stable high-energy amorphous solid dispersion of a poorly water-soluble drug. Mol Pharm. 2008;5(6):994–1002.
6. Kennedy M, Hu J, Gao P, Li L, Ali-Reynolds A, Chal B, *et al.* Enhanced bioavailability of a poorly soluble VR1 antagonist using an amorphous solid dispersion approach: a case study. Mol Pharm. 2008;5(6):981–93.
7. Albers J, Alles R, Matthée K, Knop K, Nahrup JS, Kleinebudde P. Mechanism of drug release from polymethacrylate-based extrudates and milled strands prepared by hot-melt extrusion. Eur J Pharm Biopharm. 2009;71(2):387–94.
8. Hülsmann S, Backensfeld T, Keitel S, Bodmeier R. Melt extrusion—an alternative method for enhancing the dissolution rate of 17β-estradiol hemihydrate. Eur J Pharm Biopharm. 2000;49(3):237–42.

9. Shmeis RA, Wang ZR, Krill SL. A mechanistic investigation of an amorphous pharmaceutical and its solid dispersions, part II: molecular mobility and activation thermodynamic parameters. Pharm Res. 2004;21(11):2031–9.
10. Six K, Verreck G, Peeters J, Brewster M, Van den Mooter G. Increased physical stability and improved dissolution properties of itraconazole, a class II drug, by solid dispersions that combine fast- and slow-dissolving polymers. J Pharm Sci. 2004;93(1):124–31.
11. Law D, Krill SL, Schmitt EA, Fort JJ, Qiu YH, Wang WL, *et al.* Physicochemical considerations in the preparation of amorphous ritonavir-poly(ethylene glycol) 8000 solid dispersions. J Pharm Sci. 2001;90(8):1015–25.
12. Ghebremeskel AN, Vemavarapu C, Lodaya M. Use of surfactants as plasticizers in preparing solid dispersions of poorly soluble API: stability testing of selected solid dispersions. Pharm Res. 2006;23 (8):1928–36.
13. Huang JJ, Wigent RJ, Schwartz JB. Drug-polymer interaction and its significance on the physical stability of nifedipine amorphous dispersion in microparticles of an ammonio methacrylate copolymer and ethylcellulose binary blend. J Pharm Sci. 2008;97 (1):251–62.
14. Taubner V, Shishoo R. Influence of processing parameters on the degradation of poly(L-lactide) during extrusion. J Appl Polym Sci. 2001;79:128–2135.
15. Sarraf AG, Tissot H, Tissot P, Alfonso D, Gurny R, Doelker E. Influence of hot-melt extrusion and compression molding on polymer structure organization. Investigated by Differential Scanning Calorimetry. J Appl Polym Sci. 2001;81:3124–32.
16. Andrews GP, Jones DS, Diak OA, McCoy CP, Watts AB, McGinity JW. The manufacture and characterisation of hot-melt extruded enteric tablets. Eur J Pharm Biopharm. 2008;69:264–73.
17. Bikiaris D, Papageorgiou GZ, Stergiou A, Pavlidou E, Karavas E, Kanaze F, *et al.* Physicochemical studies on solid dispersions of poorly water-soluble drugs: evaluation of capabilities and limitations of thermal analysis techniques. Thermochim Acta. 2005;439:58–67.
18. Qi S, Gryczke A, Belton P, Craig DQM. Characterisation of solid dispersions of paracetamol and EUDRAGIT® E prepared by hot-melt extrusion using thermal, microthermal and spectroscopic analysis. Int J Pharm. 2008;354(1–2):158–67.
19. Aso Y, Yoshioka S, Miyazaki T, Kawanishi T, Tanaka K, Kitamura S, *et al.* Miscibility of nifedipine and hydrophilic polymers as measured by ^{1}H-NMR spin-lattice relaxation. Chem Pharm Bull. 2007;55(8):1227–31.
20. Gao C, Stading M, Wellner N, Parker ML, Noel TR, Mills CEN, *et al.* Plasticization of a protein-based film by glycerol: a spectroscopic, mechanical, and thermal study. J Agr Food Chem. 2006;54(13):4611–6.
21. Belton PS, Hills BP. The effects of diffusive exchange in heterogeneous systems on N.M.R. line shapes and relaxation processes. Mol Phys. 1987;61:999–1018.
22. Nishi T, Wang TT. Melting-point depression and kinetic effects of cooling on crystallisation in poly (vinylidene fluoride) poly (methyl methacrylate) mixtures. Macromolecules. 1975;8:909–15.
23. Meaurio E, Zuza E, Sarasua JR. Miscibility and specific interactions in blends of poly (L-lactide) with poly(vinylphenol). Macromolecules. 2005;38:1207–15.
24. Marsac PJ, Shamblin SL, Taylor LS. Theoretical and practical approaches for prediction of drug-polymer miscibility and solubility. Pharm Res. 2006;23(10):2417–26.
25. Theeuwes F, Hussain A, Higuchi T. Quantitative analytical method for determination of drugs dispersed in polymers using differential scanning calorimetry. J Pharm Sci. 1974;63(3):427–9.
26. Gramaglia D, Conway BR, Kett VL, Malcolm RK, Batchelor HK. High speed DSC (hyper-DSC) as a tool to measure the solubility of a drug within a solid or semi-solid matrix. Int J Pharm. 2005;301:1–5.
27. Craig DQM, Newton JM. Characterisation of polyethylene glycol solid dispersions using differential scanning calorimetry and solution calorimetry. Int J Pharm. 1991;76:17–24.
28. Reading M, Craig DQM, Murphy JR, Kett VL. Modulated temperature differential scanning calorimetry. In: Craig DQM, Reading M, editors. Thermal analysis of pharmaceuticals. London: CRC; 2007. p. 103–29.
29. Srčič S, Kerč J, Urleb U, Zupančič I, Lahajnar G, Kofler B, *et al.* Investigation of felodipine polymorphism and its glassy state. Int J Pharm. 1992;87:1–10.
30. Parmar MM, Khan O, Seton L, Ford JL. Polymorph control of Felodipine form II in an attempted cocrystallization. Cryst Growth Des. 2009;9(3):1254–7.
31. Rollinger JM, Burger A. Polymorphism of racemic felodipine and the unusual series of solid solutions in the binary system of its enantiomers. J Pharm Sci. 2001;90:949–59.
32. Kerč J, Srčič S, Mohar M, Smid-Korbar J. Some physico-chemical properties of glassy felodipine. Int J Pharm. 1991; 68:25–33.
33. Flory PJ. Principles of polymer chemistry. Ithaca: Cornell University Press; 1953. p. 563–76.
34. Matsuo T. Low temperature thermal properties of amorphous materials. Pure Appl Chem. 1998;70(3):599–602.
35. Xu H, Cebe P. Heat capacity study of isotactic polystyrene: dual reversible crystal melting and relaxation of rigid amorphous fraction. Macromolecules. 2004;37(8):2797–806.
36. McBrierty VJ, Packer KJ. Nuclear magnetic resonance in solid polymers. Cambridge: Cambridge University Press; 1993. p. 52–78.